Available online at www.sciencedirect.com
SCIENCE DIRECT
New Astronomy Reviews 50 (2006) 199–203
New Astronomy Reviews
www.elsevier.com/locate/newastrev

Early metal enrichment and Lyman α emission

Masao Mori [a,b,*], Masayuki Umemura [c]

[a] Department of Physics and Astronomy, University of California, Los Angeles, CA 90095-1547, USA
[b] Institute of Natural Sciences, Senshu University, Kawasaki, Kanagawa 214-8580, Japan
[c] Center for Computational Sciences, University of Tsukuba, Tsukuba, Ibaraki 305-8577, Japan

Available online 9 January 2006

Abstract

We simulate the dynamical and chemical evolution of a forming galaxy embedded in a dark matter halo, using a three-dimensional *N*-body/hydrodynamic simulation code combined with stellar population synthesis. We find that a sparkling phase with multitudinous SN explosions at less than 3×10^8 years exhibits intense Lyman α emission from cooling shocks and well resembles Lyman α emitters (LAEs) that have been recently discovered at redshifts greater than three. Subsequently, the galaxy shifts to a stellar continuum radiation-dominated phase within 10^9 years, which appears like Lyman break galaxies (LBGs). At the LAE phase the abundance of heavy elements is subsolar and shows strong spatial variance, but it convergently reaches a level of solar abundance at the LBG phase. Hence, it turns out that LAEs and LBGs are the on-going and major phases of chemical enrichment in a galaxy.

Keywords: Hydrodynamics; *N*-body; Supernova; Star formation; Chemical evolution

Contents

1. Introduction

Recent progress in observational devices and techniques has enhanced our knowledge of formation and evolution of galaxies on a firm statistical basis. Optical observations have revealed the presence of a number of LAEs at redshifts of $z \gtrsim 3$ (Dey et al., 1998; Weymann et al., 1998; Rhoads et al., 2000; Hu et al., 2002; Ajiki et al., 2002; Dawson et al., 2002; Fujita et al., 2003; Kodaira et al., 2003; Hayashino et al., 2004) as well as LBGs at redshifts of $3 \lesssim z \lesssim 5$ (Steidel et al., 1996, 1999; Pettini et al., 2001; Giavalisco, 2002).

Recently, Ly α imaging at high-redshift revealed the existence of very luminous and extended Ly α emitters which have the Ly α luminosity of 10^{42-44} ergs s^{-1} and a physical extent of ∼100 kpc (Keel et al., 1999; Steidel et al., 2000; Matsuda et al., 2004). A good fraction of LBGs exhibit Ly α emission lines strong enough to be detected by narrow band observations (Shapley et al., 2003). Moreover, extended LAEs which are associated but not centered on known LBGs have been detected with a Ly α luminosity

* Corresponding author. Tel.: +1 310 825 4782; fax: +1 310 206 2096.
E-mail address: mmori@astro.ucla.edu (M. Mori).

1387-6473/$ - see front matter © 2005 Elsevier B.V. All rights reserved.
doi:10.1016/j.newar.2005.11.035

of $\sim 10^{43}$ erg s^{-1} at $z = 3.09$ (Steidel et al., 2000; Matsuda et al., 2004). LBGs are usually characterized by compact cores (some with multiple components) of 5–8 kpc and often surrounded by more diffuse, asymmetric halos (Steidel et al., 1996; Giavalisco et al., 1996). Since LAEs and LBGs are quite young, they could hold direct interpretable information on the early chemical enrichment of galaxies, contrary to present-day galaxies which have undergone intense interstellar medium (ISM) recycling, thus erasing most of the early chemical history.

So far, the theoretical models of galactic chemical evolution have often assumed the homogeneous ISM (one-zone model), with the instantaneous and perfect mixing of heavy elements synthesized in SNe. However, the energy input and metal ejection by SNe are likely to proceed in an inhomogeneous fashion (Tsujimoto and Shigeyama, 1998; Argast et al., 2000; Mori et al., 2004a,b; Mori and Umemura, 2006). Thus, simulations that can resolve SN remnants are required to properly model the chemical evolution of primordial galaxies. In this paper, we perform ultra-high resolution hydrodynamic simulations of a very large burst of multiple SN explosions in a forming galaxy. Also, by incorporating spectro-photometric modeling with the simulations, the results can be directly compared to the observations on high-redshift forming galaxies. The outline of this paper is as follows. In Section 2, the numerical method is described. In Section 3, we present the simulation results and in Section 4 the possible link among LAEs and LBGs is discussed.

2. Numerical method

Our simulation uses a hybrid N-body/hydrodynamics code which is applicable to a complex system consisting of dark matter, stars and gas. The gas is allowed to form stars and is subject to physical processes such as the radiative cooling and the energy feedback from SNe. The gas is assumed to be optically thin and in collisional-ionization equilibrium. Radiative cooling is included self-consistently with metallicity, using the metallicity-dependent cooling curves by Sutherland and Dopita (1993).

The collisionless dynamics for dark matter particles and stars is treated by the N-body method and the gas dynamics is pursued by a three-dimensional AUSM-DV scheme that can treat shocks with high accuracy (Mori et al., 2002). The AUSM-DV scheme proposed by Wada and Liou (1997) has a blending form of AUSM scheme developed by Liou and Steffen (1993) and flux difference scheme and improve the robustness of AUSM scheme in dealing with the collision of strong shocks. We extended it to second-order spatial accuracy using MUSCL (van Leer, 1977) with a total diminishing limiter. Since this scheme has a great advantage due to the reduction of numerical viscosity, fluid interfaces are sharply preserved and small-scale features can be resolved.

Stars are assumed to form in rapidly cooling and Jeans unstable regions at a rate which is inversely proportional to the local dynamical time (see Mori et al., 1997, 1999). When a star particle is formed, we identify this with approximately 10^4 single stars and distribute the associated mass of the star particle over the single stars according to Salpeter's initial mass function (Salpeter, 1955). The lower and upper mass limits are taken as 0.1 and 100 $M_\odot$, respectively. When a star particle is formed and identified with a stellar assemblage as described above, stars more massive than 8 $M_\odot$ start to explode as Type II SNe with the explosion energy of 10^{51} ergs and their outer layers are blown out with synthesized metals leaving the remnant of 1.4 $M_\odot$. Consequently, once a new star particle is formed, the energy, metals and material from Type II SNe are subsequently supplied to 8 cells surrounding SN region. We compute the chemical evolution using the calculations of stellar nucleosynthesis products by Tsujimoto et al. (1995). A mass of 2.4 $M_\odot$ of oxygen and of 9.05×10^{-2} $M_\odot$ of iron are ejected from a Type II SN explosion.

Chemical and photometric evolution of the system can also be simulated by this code. The emission properties of the gas components are calculated using MAPPINGIII by Sutherland and Dopita (1993), and that of the stellar components using the evolutionary stellar population synthesis code PEGASE by Fioc and Rocca-Volmerange (1997). Thus, the present simulations can be directly compared to the observations of LAEs and LBGs.

3. Simulation

Following a standard cold dark matter cosmology with cosmological constant (ΛCDM), where we assume $\Omega_M = 0.3$, $\Omega_\lambda = 0.7$, $\Omega_b = 0.04$, and a Hubble constant of $H_0 = 70$ km s^{-1} Mpc^{-1}, we consider the dynamical and chemical evolution of a protogalaxy with the total mass of 10^{11} $M_\odot$. If we suppose a 2σ density fluctuation, it decouples from the cosmic expansion and begins to contract at redshift $z = 7.8$ with the radius of 53.7 kpc. The total mass of gaseous matter is assumed to be 1.3×10^{10} $M_\odot$ initially. The angular momentum is provided by a uniform rotation characterized by a spin parameter of $\lambda \sim 0.05$ (Barnes and Efstathiou, 1987). Prior to this galaxy-scale fluctuation, subgalactic dark halos collapse and are virialized. According to the ΛCDM cosmology, twenty subgalactic condensations with mass of 5.0×10^9 $M_\odot$ and radius of 8.6 kpc are distributed within the galaxy-scale fluctuation. The subgalactic virialized halos are assumed to follow the Navarro–Frenk–White density profile (Navarro et al., 1997). The hydrodynamic processes are pursued with 1024^3 grid points. The simulation box has a physical size of 134 kpc and the spatial resolution is 0.131 kpc.

Fig. 1 represents the star formation history of the simulated galaxy. The starburst begins at $\sim 10^7$ years, and the star formation rate reaches a peak of about 40 solar mass

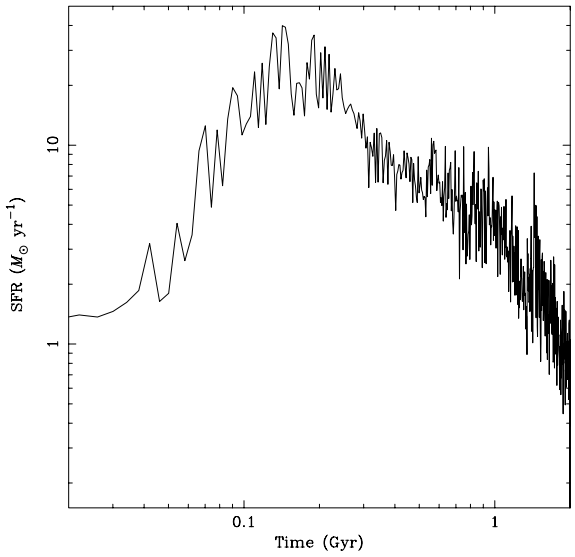

Fig. 1. Star formation history of the simulated galaxy with a unit of solar mass per year as a function of time with a unit of Gyr.

per year around 1.5×10^8 years. The burst of star formation continues until 3×10^8 years. Then, the star formation activity gradually diminishes down to a few solar mass per year after 10^9 years.

Fig. 2 shows the result for the time sequence of the chemical enrichment, where the distributions of the logarithmic density, the temperature and the velocity, and oxygen abundance [O/H], are presented until 10^9 years. In the first 10^8 years, stars are formed in high-density peaks within subgalactic condensations and the burst of star formation starts. Then, massive stars in the star forming regions explode as SNe one after another, producing expanding hot bubbles surrounded by cooled dense shells. The gas in the vicinity of SNe is quickly enriched with ejected heavy elements, but a large amount of gas still retains low heavy-element abundance. Consequently, the metallicity distribution becomes highly inhomogeneous, where gas enriched as [O/H] $\lesssim -1$ coexists with virtually primordial gas. Since the density of the ISM is lower in

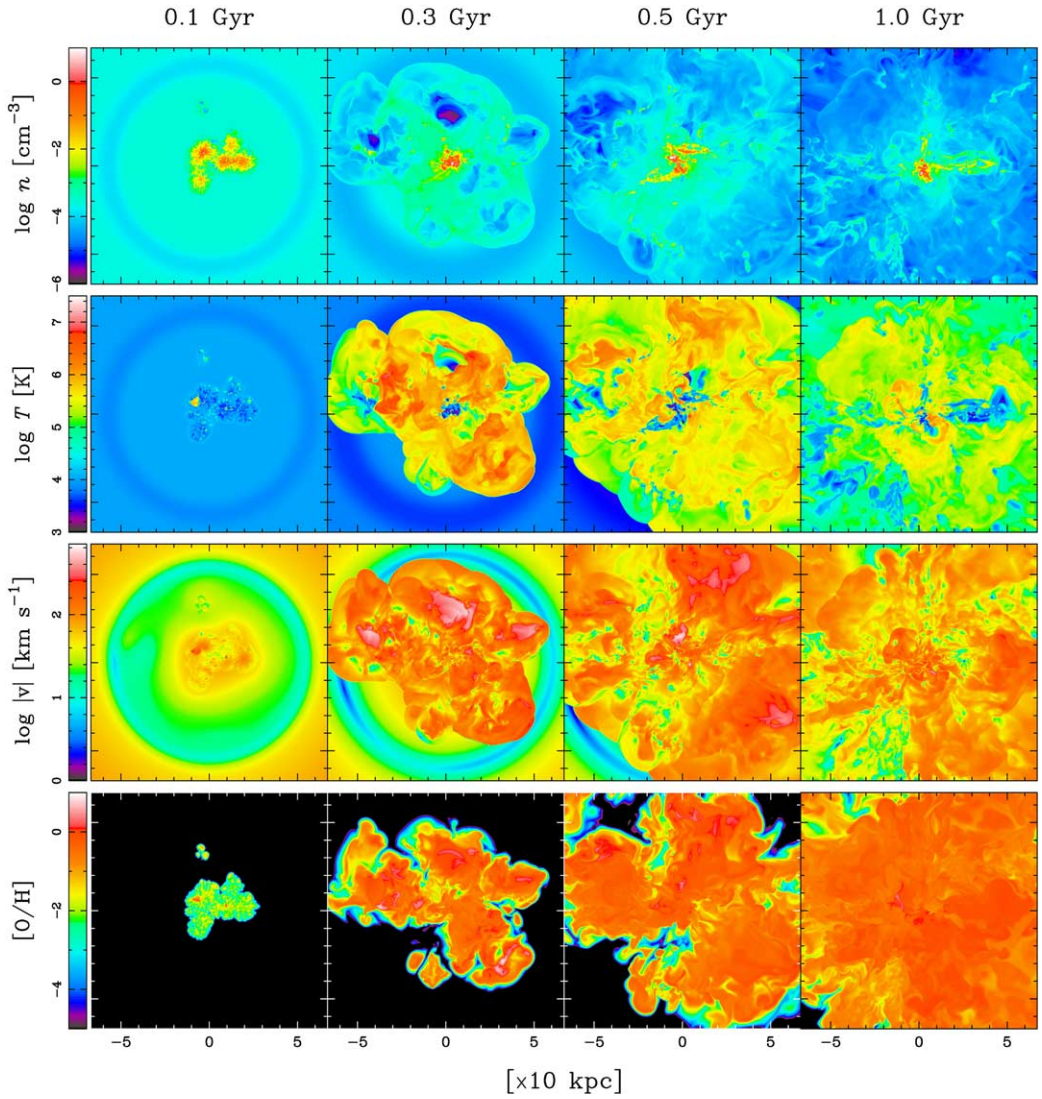

Fig. 2. Sectional distributions of the logarithmic number density of gas, the logarithmic temperature, the oxygen abundance [O/H] of gas, and projected distribution of the Ly α emission from the gas, respectively. The four panels in each low depict the time evolution of the simulation results until 1 Gyr.

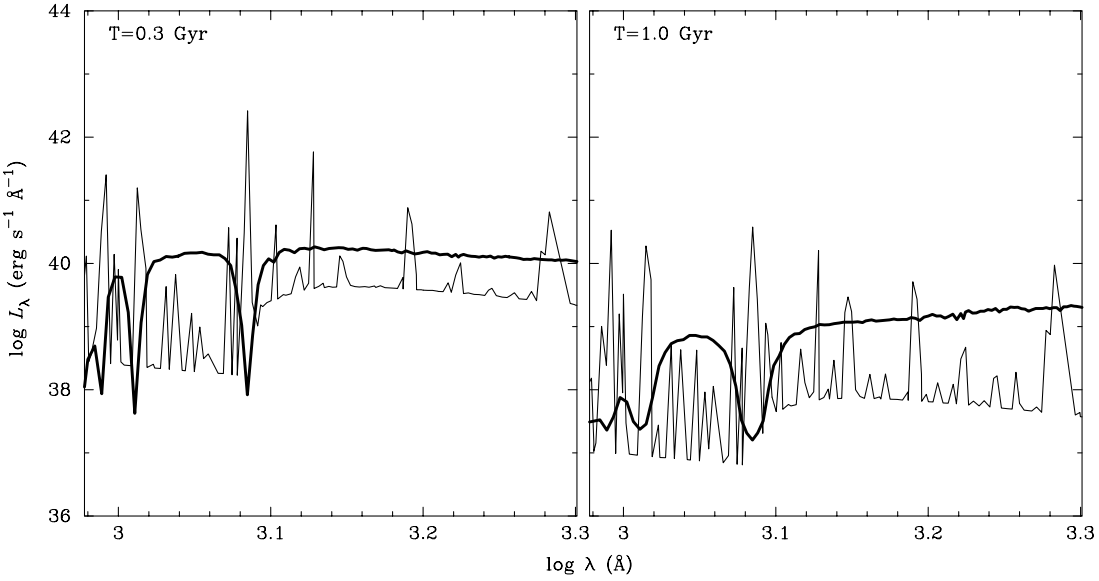

Fig. 3. Predicted spectral energy distribution of the emission from the simulated galaxy. The emission properties of the gas components assuming for an optically thin gas in collisional-ionization equilibrium (thin lines), and that of the stellar components using the evolutionary stellar population synthesis (thick lines). Here, the luminosities of line emissions are average over bin. The absolute luminosities of Ly α line emission, where the wave length is 1216 Å, are 1.6×10^{43} and 2.3×10^{41} erg s^{-1} at the elapsed time of 0.3 and 1 Gyr, respectively.

the outer regions of subgalactic condensations, the expansion of hot bubbles is accelerated there and supernova-driven shocks collide with each other to generate super-bubbles of ~50 kpc, and the surrounding high-density, cooled ($T = 10^4$ K) shells form at 3×10^8 years. The hot bubbles expand further by subsequent SN explosions, and the shells sweep up the partially enriched ambient gas. The gas density in dense shells increases owing to the efficient radiative cooling mainly through collisional excitation of neutral hydrogen.

After 5×10^8 years, the hot bubbles blow out into the intergalactic space. This supernova-driven outflow is an efficient mechanism to enrich the intergalactic medium with heavy elements over a large cosmological volume (see Mori et al., 2002). On the other hand, the dense shells undergoes hydrodynamic instabilities induced by shell–shell interactions and radiative cooling, eventually fragmenting into cold filaments and blobs. These interactions are giving rise to an intricate multiphase structure in the inner halo, where 10^{6-7} K gas coexists with a cooler 10^4 K phase from which it is separated by cooling interfaces. New stars are born in this enriched gas and again heavy elements are ejected from subsequent SNe. The rightmost panels show the structure at 1 Gyrs. By this stage, the ISM is recycled repeatedly and about 72% of the initial gas has been processed into stars. Eventually, some amounts of cool, dense filaments are left at the center. But, the most of volume is filled with rarefied gas ($n \lesssim 10^{-4}$ cm^{-3}) that has intermediate temperature ($10^{4.5}$ K $\lesssim T \lesssim 10^{6.5}$ K). At this epoch, the mixing of heavy elements is nearly completed.

Fig. 3 shows the spectral energy distribution (SED) of the simulated galaxy. In practice, to obtain the SED of the system we sum up the SED of each grid point for the gas components and each star particle for stellar components. In this figure, thin lines and thick lines depict, respectively, the gas emission and the stellar emission. The Ly α emission comes mainly from high-density cooling shells, and its luminosity is more than 10^{43} erg s^{-1} in the first 3×10^8 years. This Ly α luminosity perfectly matches that of observed LAEs (Matsuda et al., 2004; Tanighichi et al., 2005). After 3×10^8 years, the Ly α luminosity quickly declines to several 10^{41} erg s^{-1} that is lower than the observed level. This result suggests that LAEs can correspond to an early supernova-dominated phase before 3×10^8 years.

4. Summary and discussion

Ultra-high resolution hydrodynamic simulations using 1024^3 grid points are performed of a very large SN burst in a forming galaxy, with properties similar to those inferred for LAEs. We find that the bubbly structure produced by multiple SNe are quite similar to the observed features in Ly α surface brightness distributions of LAEs. Since LAEs correspond to a quite early phase of galaxy chemical evolution, the observed bubbly features imply that the self-enrichment is on-going in a very inhomogeneous fashion in LAEs.

As seen in Fig. 3, after the sparkling phase of a primeval galaxy, the SED is dominated by stellar continuum emission, since the emission from cooling gas decreases immediately owing to the leak of explosion energy through the blowout of super-bubbles. The galaxy in this phase is featured with diffuse, asymmetric structures, and outflows of $100 \sim 500$ km s^{-1} (see Fig. 2). These features look quite similar to those observed for LBGs (Adelberger et al.,

2002), where the low-ionization interstellar absorption lines of LBGs are blueshifted by hundreds km s^{-1} relative to systemic velocities and Ly α lines are redshifted to the same degree.

In the light of such properties, the simulated post-starburst galaxy that has the age of $\sim 10^9$ years can correspond to LBGs. These comparisons of the simulation results with the observations allow us to derive a significant conclusion that LAEs are progenitors of LBGs, and the on-going, major chemical enrichment phases.

Acknowledgements

This work was supported in part by the Grant-in-Aid of the JSPS, 14740132, and by Grants-in-Aid for Scientific Research from the Ministry of Education, Culture, Sports, Science, and Technology (MEXT), 16002003. The computations reported here were performed on the Earth Simulator at the JAMSTEC in Yokohama, Japan, and the SPACE at the Institute of Natural Sciences, Senshu University in Kawasaki, Japan.

References

Adelberger, K.L., Steidel, C.C., Shapley, A.E., Pettini, M., 2002. ApJ 584, 45.
Ajiki, M. et al., 2002. ApJ 576, L25.
Argast, D., Samland, M., Gerhard, O.E., Thielemann, F.-K., 2000. A&A 356, 873.
Barnes, J., Efstathiou, G., 1987. ApJ 319, 575.
Dawson, S., Spinrad, H., Stern, D., Dey, A., van Breugel, W., de Vries, W., Reuland, M., 2002. ApJ 570, 92.
Dey, A., Spinrad, H., Stern, D., Graham, J.R., Chaffee, F.H., 1998. ApJ 498, L93.
Fioc, M., Rocca-Volmerange, B., 1997. A&A 326, 950.
Fujita, S.S. et al., 2003. AJ 125, 13.
Giavalisco, M., 2002. ARA&A 40, 579.
Giavalisco, M., Steidel, C.C., Macchetto, F.D., 1996. ApJ 470, 189.
Hayashino, T. et al., 2004. AJ 128, 2073.
Hu, E.M., Cowie, L.L., McMahon, R.G., Capak, P., Iwamuro, F., Kneib, J.-P., Maihara, T., Motohara, K., 2002. ApJ 568, L75.
Keel, W.C., Cohen, S.H., Windhorst, R.A., Waddington, I., 1999. AJ 118, 2547.
Kodaira, K. et al., 2003. PASJ 55, L17.
Liou, M.-S., Steffen, C.J., 1993. J. Comput. Phys. 107, 23.
Matsuda, Y. et al., 2004. AJ 128, 569.
Mori, M., Ferrara, A., Madau, P., 2002. ApJ 571, 40.
Mori, M., Umemura, M., Ferrara, A., 2004a. ApJ 613, 97.
Mori, M., Umemura, M., Ferrara, A., 2004b. PASA 21, 232.
Mori, M., Umemura, M., 2006. Nature, in press.
Mori, M., Yoshii, Y., Nomoto, K., 1999. ApJ 511, 585.
Mori, M., Yoshii, Y., Tsujimoto, T., Nomoto, K., 1997. ApJ 478, L21.
Navarro, J.F., Frenk, C.S., White, S.D.M., 1997. ApJ 490, 493.
Pettini, M., Shapley, A.E., Steidel, C.C., Cuby, J., Dickinson, M., Moorwood, A.F.M., Adelberger, K.L., Giavalisco, M., 2001. ApJ 554, 981.
Rhoads, J.E., Malhotra, S., Dey, A., Stern, D., Spinrad, H., Jannuzi, B.T., 2000. ApJ 545, 85.
Salpeter, E.E., 1955. ApJ 121, 161.
Shapley, A.E., Steidel, C.C., Pettini, M., Adelberger, K.L., 2003. ApJ 588, 65.
Steidel, C.C., Adelberger, K.L., Giavalisco, M., Dickinson, M., Pettini, M., 1999. ApJ 519, 1.
Steidel, C.C., Adelberger, K.L., Shapley, A.E., Pettini, M., Dickinson, M., Giavalisco, M., 2000. ApJ 532, 170.
Steidel, C.C., Giavalisco, M., Dickinson, M., Adelberger, K.L., 1996. AJ 112, 352.
Sutherland, R.S., Dopita, M.A., 1993. ApJS 88, 253.
Tanighichi, Y. et al., 2005. PASJ 57, 165.
Tsujimoto, T., Nomoto, K., Yoshii, Y., Hashimoto, M., Yanagida, S., Thielemann, F.-K., 1995. MNRAS 277, 945.
Tsujimoto, T., Shigeyama, T., 1998. ApJ 508, L151.
van Leer, B., 1977. J. Comput. Phys. 32, 104.
Wada, Y., Liou, M.-S., 1997. SIAM J. Sci. Comput. 18, 633.
Weymann, R.J., Stern, D., Bunker, A., Spinrad, H., Chaffee, F.H., Thompson, R.I., Storrie-Lombardi, L.J., 1998. ApJ 505, L95.